

Photon stimulated desorption from a vacuum chamber at the National Synchrotron Light Source

T. Kobari and H. J. Halama

Citation: *Journal of Vacuum Science & Technology A* **5**, 2355 (1987); doi: 10.1116/1.574451

View online: <http://dx.doi.org/10.1116/1.574451>

View Table of Contents: <http://scitation.aip.org/content/avs/journal/jvsta/5/4?ver=pdfcov>

Published by the AVS: Science & Technology of Materials, Interfaces, and Processing

Articles you may be interested in

[Experiences from nonevaporable getter-coated vacuum chambers at the MAX II synchrotron light source](#)

J. Vac. Sci. Technol. A **28**, 220 (2010); 10.1116/1.3281432

[Photon stimulated desorption from copper and aluminum chambers](#)

J. Vac. Sci. Technol. A **25**, 1251 (2007); 10.1116/1.2712187

[Vacuum chamber for the wiggler of the Taiwan Light Source at the Synchrotron Radiation Research Center](#)


J. Vac. Sci. Technol. A **14**, 2624 (1996); 10.1116/1.579990

[Gas desorption from an oxygen free high conductivity copper vacuum chamber by synchrotron radiation photons](#)

J. Vac. Sci. Technol. A **12**, 846 (1994); 10.1116/1.579265


[Vacuum system for national synchrotron light source](#)

J. Vac. Sci. Technol. **16**, 720 (1979); 10.1116/1.570067



Instruments for Advanced Science

Contact Hiden Analytical for further details:
W www.HidenAnalytical.com
E info@hiden.co.uk
[CLICK TO VIEW](#) our product catalogue




Gas Analysis

- › dynamic measurement of reaction gas streams
- › catalysis and thermal analysis
- › molecular beam studies
- › dissolved species probes
- › fermentation, environmental and ecological studies



Surface Science

- › UHV TPD
- › SIMS
- › end point detection in ion beam etch
- › elemental imaging - surface mapping



Plasma Diagnostics

- › plasma source characterization
- › etch and deposition process reaction
- › kinetic studies
- › analysis of neutral and radical species



Vacuum Analysis

- › partial pressure measurement and control of process gases
- › reactive sputter process control
- › vacuum diagnostics
- › vacuum coating process monitoring

Photon stimulated desorption from a vacuum chamber at the National Synchrotron Light Source

T. Kobari

MERL, Hitachi Ltd., Kandatsu, Tsuchiura, Ibaraki, 300 Japan

H. J. Halama

Brookhaven National Laboratory, Upton, New York 11973

(Received 18 September 1986; accepted 17 November 1986)

In our search for surfaces exhibiting the lowest photon stimulated desorption, we have exposed a 3-m-long beam tube to photons from the vacuum ultraviolet ring of the National Synchrotron Light Source having critical energy of ~ 500 eV. Desorption of H_2 , CH_4 , CO, and CO_2 , which are the main gas species, was studied as a function of the beam dose for the following surface treatments: standard chemical cleaning, Ar 10% O_2 glow discharge, N_2 glow discharge, and radio frequency glow discharge using O_2 disassociation. In addition, we measured the desorption as a function of vertical collimator position. N_2 glow discharge treatment yielded the lowest desorption.

I. INTRODUCTION

Photon stimulated desorption (PSD) due to circulating electron or positron beams is responsible for most of the gas load in storage rings. The attainment of sufficiently low pressure is essential for long lifetimes at high current which is the most important characteristic of a well-operating machine. A machine designer can either provide a large pumping speed which is expensive, and in some cases difficult due to space restrictions, or attempt to lower the desorption by a suitable surface treatment. In particular, the desorption of the heavier gases has the most detrimental effect on beam lifetime. We have, therefore, exposed a 3-m-long vacuum chamber to synchrotron radiation from the vacuum ultraviolet (VUV) ring and have measured the desorption for several surface treatments commonly used in accelerator laboratories. The details of this study are described below. In the near future, we will also study a coextruded chamber and a chamber with thin TiN coating.

II. EXPERIMENTAL SETUP

The experimental setup consisting of the beam line and the test chamber (aluminum extrusion) connected through a double bellow to a stainless chamber in which a calibrated mass spectrometer and a Bayard-Alpert (BA) gauge are installed is shown in Fig. 1. The synchrotron light is collimated to 4.5 mrad in the vertical and 4 mrad in the horizon-

tal plane by two collimators C_V and C_H . In a bending magnet, most of synchrotron radiation is contained in a narrow cone having a nominal angular spread of $1/\gamma$ (Refs. 1 and 2), where $\gamma = E/\text{electron rest energy} = 750/0.511 = 1468$, (VUV ring). The $1/\gamma$ represents an angle of 0.7 mrad which is much smaller than the collimation angle of 4.5 mrad chosen in our experiment. In addition, all excluded photons represent only 0.2% of total radiation power and their effect on PSD is smaller than our experimental and calibration errors. The incidence angle of 8.7 mrad is chosen to expose 2.6 m of the test chamber without exposing the orifice and the stainless chamber. Thus, 1.1 W m^{-2} of radiation power is incident on 800 cm^2 of the chamber for 300 mA of beam current.

The system is pumped down by two ion pumps and a titanium sublimation pump and the total pumping speed is more than 1500 l s^{-1} for CO. Since the conductance from the orifice 01 to the orifice 02 is 47 l s^{-1} , which is much smaller than the pumping speed, the 47 l s^{-1} can be regarded as the pumping speed at orifice 02.

III. ACCUMULATED PHOTONS AND MOLECULAR DESORPTION YIELD

The total incident photon flux per beam current I , per horizontal opening angle θ , and per second t is given by³

$$N/I\theta t = 1.28 \times 10^{14} E \text{ photons mA}^{-1} \text{ mrad}^{-1} \text{ s}^{-1}, \quad (1)$$

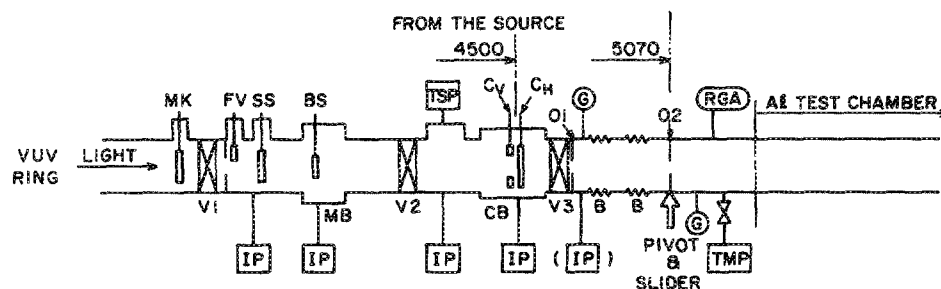


FIG. 1. Schematic diagram of the beam line and the test chamber: B—bellows, C_V and C_H —collimator, 01 and 02—orifice.

where E is the machine energy of 0.75 GeV. Since the main gases caused by PSD are H_2 , CH_4 , CO , and CO_2 , the residual gas analyzer (RGA) was calibrated to yield their relative sensitivities. The absolute partial pressures have always been calculated from the calibrated BA gauge reading. The relative abundance of desorbed gases is obtained from RGA data. The RGA was recalibrated every time the test chamber was disconnected from the beam line. The specific molecular desorption yield η_i is given by

$$\eta_i = \frac{GS_i \Delta P_i / I}{(N / I \theta t) \theta_i} \text{ molecules photon}^{-1}, \quad (2)$$

where $\Delta P_i / I$ is the specific pressure rise of each gas in Torr mA^{-1} , θ_i is the horizontal opening angle in the experiment, $G = 3.2 \times 10^{19}$ molecules Torr $^{-1}$ l $^{-1}$, S_i is the pumping speed in l s $^{-1}$ for each gas species at orifice 02.

IV. RESULTS AND DISCUSSION

A. Treatment and history of the test chamber

The test chamber was a section of actual National Synchrotron Light Source (NSLS) aluminum extrusion (6063-T5). The same test chamber, which received six different surface treatments, was used in all six experimental runs. After each surface treatment the test chamber was filled with liquid-nitrogen (LN_2) boiloff and transported to the beam line. Then it was assembled into the beam line, evacuated, and baked out for 24 h at 150 °C. The following surface treatments were performed:

Run 1: NSLS standard cleaning (caustic etch); total beam dose (TBD) = 27.6 A h.

Run 2: Venting to air for three weeks; 90% Ar + 10% O_2 glow discharge (4×10^{17} ions cm^{-2}) with bakeout (140 °C \times 24 h); TBD = 37.4 A h.

Run 3: Venting to air for 4 h; TBD = 13.6 A h.

Run 4: Venting to air for 3 d (including venting to CO_2 and CO , each for 4 h); 90% Ar + 10% O_2 glow discharge (4×10^{17} ions cm^{-2}); N_2 glow discharge (3.3×10^{17} ions cm^{-2}); TBD = 34.7 A h.

Run 5: Venting to air for 1 d and venting to CO for 2 d; O_2 rf disassociation for 26 h; TBD = 29.9 A h.

Run 6: Venting to air for 1 d; *in situ* bakeout; *in situ* O_2 rf disassociation for 40 h; TBD = 17.1 A h.

The background pressures after *in situ* bakeout were $1-3 \times 10^{-9}$ Torr except for run 3 (1×10^{-8}) due to inadequate bakeout.

B. Molecular desorption yield

Desorption yields are obtained through the specific pressure rise $\Delta P / I$ measured as a function of electron beam dose during the experiment. Since $\Delta P / I$ depends on the photon flux and the pumping speed, we derive the molecular desorption yield η , which is independent of them in order to compare our results with others.^{3,4} The beam dose of 160 A h was accumulated in the test chamber throughout the experiment. The total gas desorbed is obtained by integrating the specific pressure rise which is normalized by the beam current as a function of beam dose. Since one monolayer con-

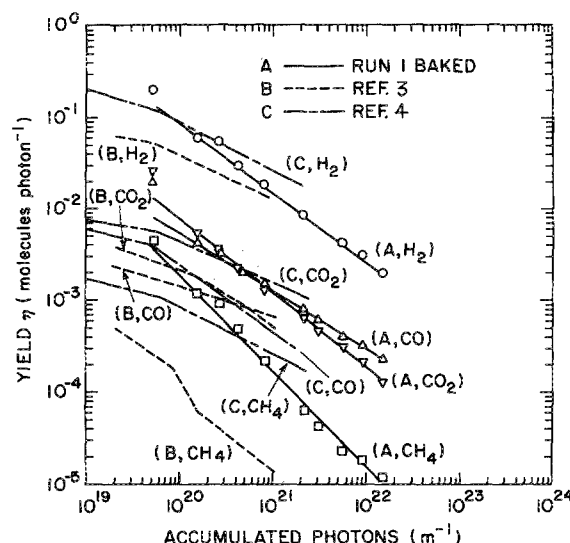


FIG. 2. Comparison of run 1 desorption yields vs accumulated photons with two other experiments (Refs. 3 and 4).

tains about 5×10^{14} molecules cm^{-2} , 0.12 Torr l corresponds to one monolayer desorbed from the test chamber.

The run 1 molecular desorption yields are shown in Fig. 2 as A. For comparison, we also plot the results obtained on baked aluminum chambers: B by Gröbner *et al.*³ at DCI, and C by the SSC CDG⁴ at NSLS. Even though the accumulated photons in Fig. 2 are identical, the photon energy spectrum of B is quite different from those of both A and C. The critical energy of B is 3 keV, and those of A and C are 0.5 keV. This might be the main reason that B gives the lowest desorption yields. In addition, the difference in desorption yield could be attributed to different background pressures, different Al alloys, and pretreatments, as well as different angles of incidence, which were 8.7, 11, and 10 mrad, respectively. The dynamic pressure rise of H_2O was very small in all six runs. More than 10^{22} photons m^{-1} were accumulated

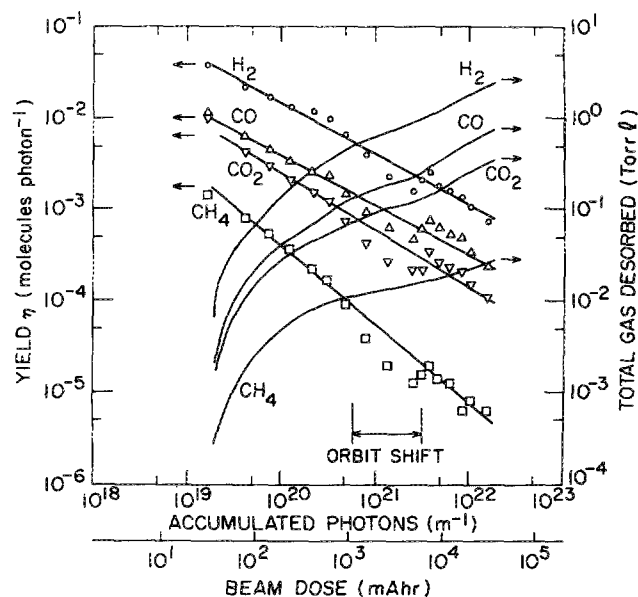


FIG. 3. Run 2: Molecular desorption yields and total gas desorbed vs beam dose.

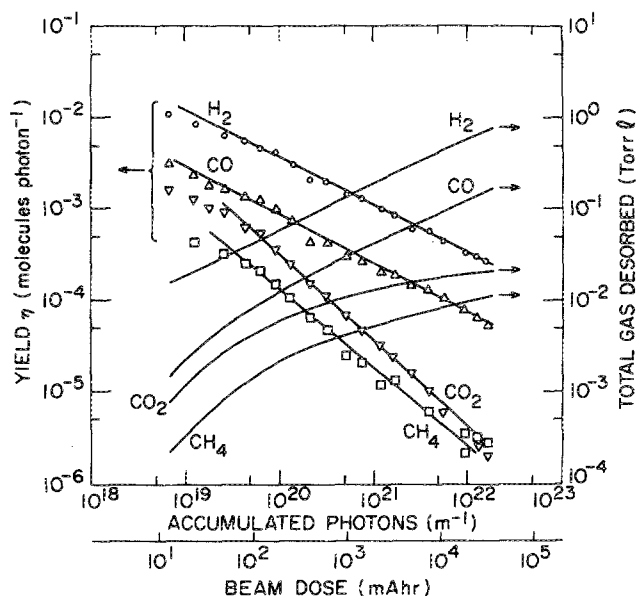


FIG. 4. Run 4: Molecular desorption yields and total gas desorbed vs beam dose for run 4.

by the end of run 1 and the yields still showed exponential decay for the four measured gases.

The molecular desorption yields and the total gas desorbed for run 2, run 4, and run 5 are shown in Figs. 3–5. We note that the yields of CH_4 are the lowest and those of H_2 are the highest in all runs. The slope change in Fig. 3 at 10^3 mA h was caused by vertical orbit shift which decreased the photon flux incident on the chamber. Upon orbit correction, normal behavior was restored. It is interesting that the slopes of CH_4 , CO , and CO_2 for run 3 are almost the same as those for run 1, except for H_2 . The total H_2 gas desorbed by the same beam dose of 1×10^{21} photons m^{-2} differs significantly in both runs; 3 Torr ℓ (25 monolayers) in run 1, but only 0.35 Torr ℓ (3 monolayers) in run 3. Since the data do not differ

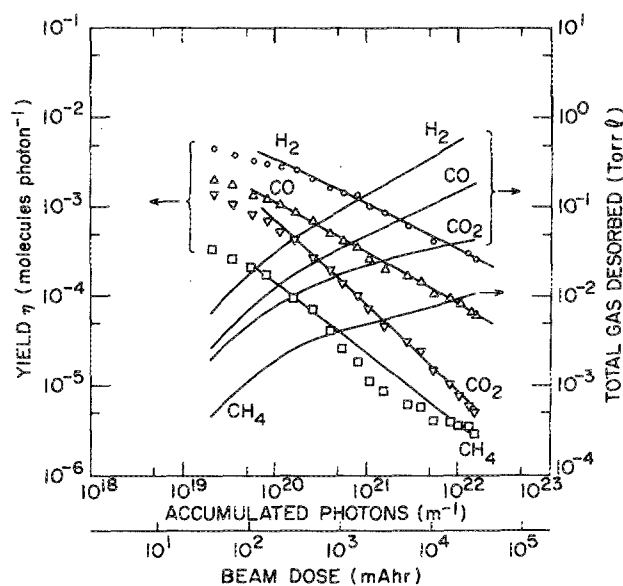


FIG. 5. Run 5: Molecular desorption yields and total gas desorbed vs beam dose for run 5.

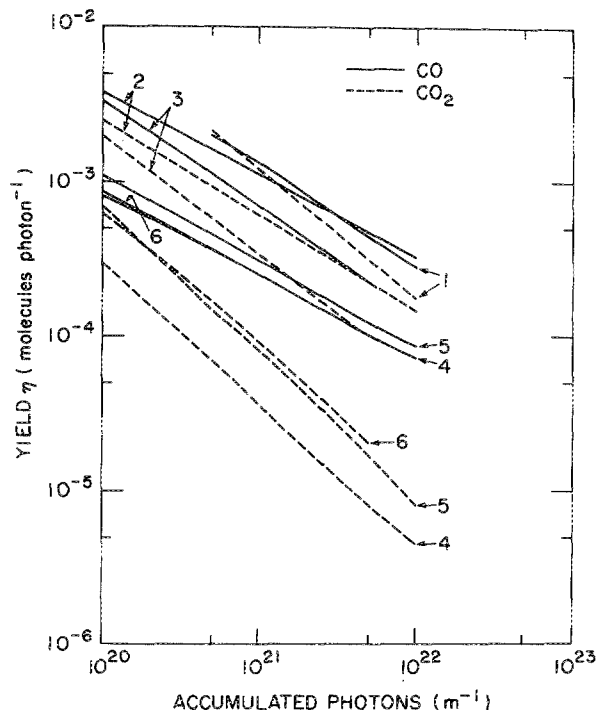


FIG. 6. Comparison of CO and CO_2 yields for experimental runs 1–6.

significantly from run 2, the plots of run 3 are not included.

Since CO and CO_2 influence the beam lifetime most drastically,⁵ we compare their desorption yields in Fig. 6. The most dramatic improvement took place after N_2 glow discharge (run 4). It was expected that some chemical compounds might form in this process and reduce both photoelectron yield^{6,7} and PSD. Since the chamber had already been exposed to photons for 78.6 A h during previous runs, we might expect some beam cleaning. However, after fully venting to air, glow discharge treatment would be expected to change the surface conditions much more drastically than the memory effect of beam cleaning.

The O_2 rf disassociation pretreatment (Fig. 5) was investigated because it has been used successfully to clean contamination of the optical components at the NSLS beam lines. After run 4 the slopes of the yields for all gases are almost the same, which may indicate a permanent memory effect of N_2 glow discharge and its change in surface structure.

C. Beam lifetime

Beam lifetimes⁵ due to bremsstrahlung and coulomb scattering for each run were obtained from the specific pressure rise and shown in Fig. 7. These lifetimes are calculated using the measured values of four gases. Even though photon flux density and pumping speed differ from actual ring conditions, the effect of each treatment on the lifetime can be clearly seen in Fig. 7.

D. Beam and desorption profile

In order to determine the desorption effectiveness of various photon intensities, a horizontal slit 1.3 mm high and a horizontal wire were traversed through a white light beam

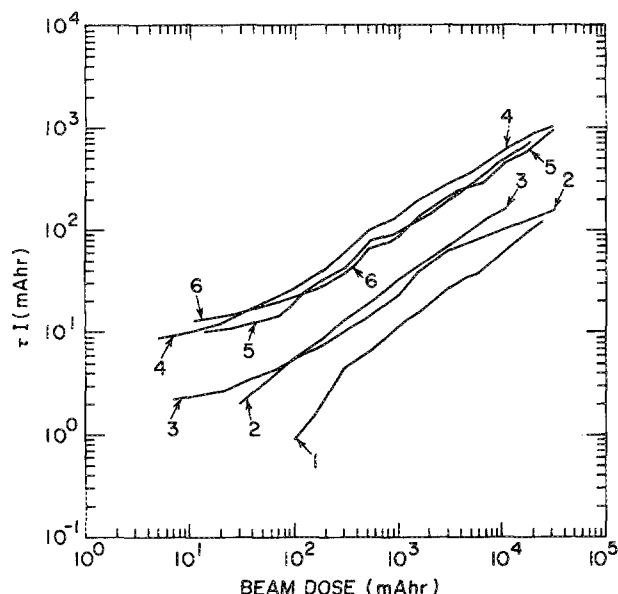


FIG. 7. Beam lifetimes vs beam dose.

vertically from $a = 0$ mm to $a = 10$ mm which corresponds to the vertical half-angle of 2.2 mrad (see Fig. 8). Both the desorption and the photoelectron current were measured and are plotted in Fig. 8 normalized by values at the center of the beam. The profiles obtained by these two measurements are in good agreement and show that desorption is proportional to photocurrent intensity. For a collimator position of $a = 6$ mm, which corresponds to a vertical half-angle of 1.3 mrad, the desorption is 20% of the maximum and gas desorption caused by the photons within ± 1.3 mrad is more than 80% of all desorption.

V. CONCLUSIONS

Since the same chamber was used during the entire experiment some memory effect influencing later runs cannot be excluded. However, from experience with real machines, exposure to laboratory air undoes much of the beneficial effects of beam cleaning. The following conclusions are drawn from our investigation: (1) N_2 glow discharge (run 4) results in the lowest desorption and the slope of CO_2 yields versus beam dose curve becomes steeper. (2) Permanent slope change after N_2 glow discharge may indicate a permanent change in surface structure. (3) rf glow discharge is a good

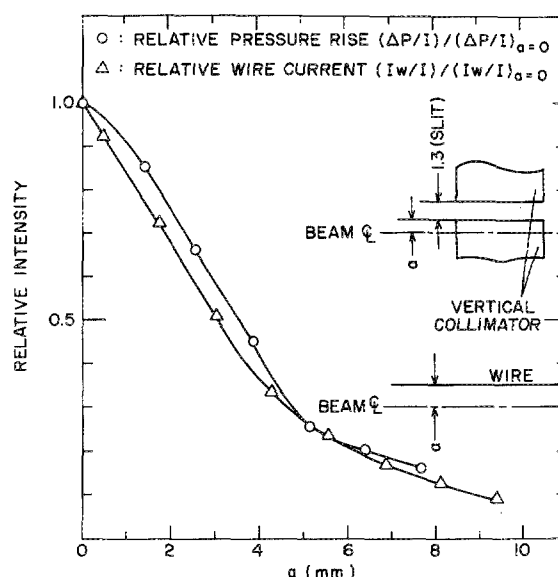


FIG. 8. Relative pressure and photocurrent vs distance from beam center.

method to remove surface contamination but the result may be enhanced by previous N_2 glow discharge. (4) A combination of Ar and N_2 glow discharges appears to be the most effective method to enhance the lifetime.

ACKNOWLEDGMENTS

We thank C. Lanni and the NSLS Vacuum Group for their excellent technical support and measurements. The guidance of rf disassociation by E. Johnson is also appreciated. This work performed under the auspices of the U. S. Department of Energy.

¹*X-Ray Data Booklet*, edited by D. Vaughan (Lawrence Berkeley Laboratory, Berkeley, CA, 1986).

²W. C. Mead, E. M. Campbell, K. G. Estabrook, R. E. Turner, W. L. Kruer, P. H. Y. Lee, B. Pruett, V. C. Rupert, K. G. Tircell, G. L. Stradling, F. Ze, C. E. Max, M. D. Rosen, and B. F. Lasinski, *Phys. Fluids* **26**, 2316 (1983).

³O. Gröbner, A. G. Mathewson, H. Stör, and P. Strubin, *Vacuum* **33**, 397 (1983).

⁴H. Jostlein, D. Trebojevic, D. Bintinger, and P. Limon, NSLS Annual Report No. BNL-51947 UC-13, 1985, p. 124.

⁵H. Halama, *J. Vac. Sci. Technol. A* **3**, 1699 (1985).

⁶J. Kouptsidis and A. G. Mathewson, DESY 76/49, 1976.

⁷A. G. Mathewson, G. Horikoshi, and H. Mizuho, KEK-78-9, 1978.